

# Cosmic ray measurements from Voyager 2 as it crossed into interstellar space

Edward C. Stone<sup>1\*</sup>, Alan C. Cummings<sup>1</sup>, Bryant C. Heikkilä<sup>2</sup> and Nand Lal<sup>2</sup>

**The interaction of the interstellar and solar winds is complex, as revealed by differences in intensities and anisotropies of low-energy ions (>0.5 MeV per nucleon) originating inside the heliosphere and those of higher-energy Galactic cosmic rays (>70 MeV per nucleon) originating outside, in the Milky Way. On 5 November 2018, Voyager 2 observed a sharp decrease in the intensity of low-energy ions and a simultaneous increase in the intensity of cosmic rays, indicating that Voyager 2 had crossed the heliopause at 119 au and entered interstellar space about six years after Voyager 1. Unlike Voyager 1, which found that two interstellar flux tubes had invaded the heliosheath and served as precursors to the heliopause, Voyager 2 found no similar precursors. However, just beyond the heliopause Voyager 2 discovered a boundary layer, in which low-energy particles streamed outward along the magnetic field and cosmic ray intensities were only 90% of those further out.**

On 25 August 2012, Voyager 1 crossed the heliopause, the contact surface separating the solar and interstellar winds, and entered interstellar space at 121.6 au (refs. 1–3). There was no direct measurement of the solar wind or interstellar wind plasmas as Voyager 1 transitioned from the heliosheath, the outermost layer of the heliosphere, to the Very Local Interstellar Medium (VLISM), since the plasma instrument (PLS) is not working. Despite the lack of direct plasma measurements, there were other signatures that Voyager 1 crossed the heliopause, such as expected differences in the heliospheric and interstellar magnetic field strengths<sup>1</sup>. However, the direction of the magnetic field was the same as that of the heliospheric field, not the direction expected in the VLISM. Fortunately, on 9 April 2013 a solar transient excited electron plasma oscillations that indicated an electron density of  $0.08\text{ cm}^{-3}$ , confirming that Voyager 1 was in the VLISM<sup>3</sup>.

The heliopause region is complex, as seen in Fig. 1. As Voyager 1 approached the heliopause, it encountered two precursor flux tubes with increased magnetic fields<sup>2</sup>, increased cosmic ray intensities and reduced intensities of low-energy heliospheric ions, suggesting that interstellar flux tubes had crossed the heliopause and invaded the heliosheath<sup>4,6</sup>. Pitch angle anisotropies in the flux tubes indicated that low-energy ions streaming outward along the magnetic field were depleted the most<sup>4</sup>.

The heliopause region is dynamic and responsive to dynamical processes in the solar wind. Magnetohydrodynamic models of the complex interaction of the solar wind and the VLISM reveal the transport of denser VLISM plasma across the heliopause caused by turbulence near the heliopause<sup>7,8</sup>. Hybrid simulations that combine cosmic ray transport and magnetohydrodynamic models<sup>9</sup> reveal the possibility of cosmic ray modulation beyond the heliopause, while other simulations<sup>10</sup> exhibit a region with limited modulation within 10 au of the heliopause, with a modulation level that varies with the magnitude of diffusion parallel and perpendicular to the magnetic field in the outer heliosheath. Although Voyager 1 did not observe significant modulation beyond the heliopause<sup>11</sup>, Voyager 2 observed a thin region like this close to the heliopause.

Voyager 1 crossed the region following a five-year period of slow inward motion of the heliopause, while six years later Voyager 2 had been pursuing an outward moving heliopause during a period of

declining solar activity<sup>12</sup>. In addition, Voyager 1 was at  $35^\circ\text{ N}$  solar ecliptic latitude and Voyager 2 was at  $37^\circ\text{ S}$  and  $35^\circ$  closer to the flank of the heliosphere, probably meaning important differences between the local internal and external conditions. Voyager 2 observations<sup>13–16</sup> will greatly aid our understanding of the interaction of the solar and interstellar winds, since Voyager 2 is a unique probe of the heliopause south of the ecliptic plane. The direct measurements of the solar and interstellar winds<sup>16</sup> are of special importance, revealing that Voyager 2 crossed the heliopause and began observing VLISM plasma on 5 November 2018.

## Results

The data used in this investigation are from the Cosmic Ray Subsystem (CRS)<sup>17</sup>, which consists of seven cosmic ray telescopes, two of which are double ended. The Electron Telescope (TET) is devoted to measuring electrons with  $\sim 2\text{--}100\text{ MeV}$ . There are four, essentially identical, Low-Energy Telescopes (LETs), designated LET A, LET B, LET C and LET D, which are mounted such that the boresights of LET A, LET B and LET D form an orthogonal system, and the boresight of LET C is opposite to that of LET A. These four telescopes measure ions with nuclear charge  $Z=1\text{--}28$ . The lowest energy recorded from these telescopes is  $\sim 0.5\text{ MeV}$  and is from protons depositing  $\sim 0.2\text{ MeV}$  or more in the front silicon solid-state detector, designated LA1, LB1, LC1 and LD1. The two double-ended telescopes are the High-Energy Telescopes (HETs), designated HET 1 and HET 2, with A and B used to refer to the entrance end of a telescope for the particles. These telescopes measure electrons with  $2.7\text{--}14.2\text{ MeV}$  and also ions with  $Z=1\text{--}28$ . More information about these telescopes can be found in Methods.

In Fig. 1 we show an overview of the heliopause crossings of Voyager 1 and Voyager 2 from the cosmic ray perspective based on data from the CRS<sup>17</sup>, in which we have shifted the Voyager 1 observations to approximately align the times of the crossings of the heliopause.

Fig. 1a,c shows rates that are dominated by Galactic cosmic rays (GCRs), with nuclei in Fig. 1a and electrons in Fig. 1c. Fig. 1b shows a rate that before the crossings is due to anomalous cosmic rays (ACRs)<sup>18,19</sup> that are accelerated somewhere in the heliosheath, but after the crossings eventually plateaus at a rate,  $\sim 2\text{ s}^{-1}$ , which is due

<sup>1</sup>California Institute of Technology, Pasadena, CA, USA. <sup>2</sup>NASA/Goddard Space Flight Center, Greenbelt, MD, USA. \*e-mail: [ecs@srl.caltech.edu](mailto:ecs@srl.caltech.edu)

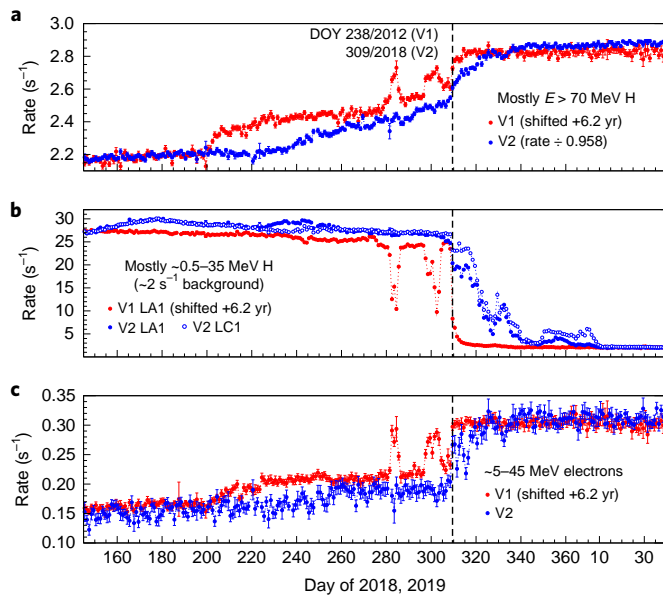


**Fig. 1 | Counting rates of different energetic particle species on Voyager 1 and Voyager 2 around the times of their crossings of the heliopause.**

All rates represent daily averages. Error bars represent  $\pm 1$  s.d. DOY, day of year. **a**, Rate from particles penetrating HET 2 on Voyager 1 (V1) and HET 1 on Voyager 2 (V2). GCR nuclei and electrons contribute to these rates, but they are dominated by protons with  $>70$  MeV (ref. <sup>11</sup>). The Voyager 1 rate is the same as the rate presented in Fig. 1 of Cummings et al.<sup>11</sup>, except for a different time period. The time plotted for Voyager 1 is the actual time plus 6.2 yr to approximately align the times of the crossings of the heliopause, which is shown by the vertical dashed line. The Voyager 2 rate has been divided by 0.958 on the basis of an intercalibration that took place in 1977–78 when the two spacecraft were close together in space. In the VLISM, the Voyager 2 rate is about 2% higher than that of Voyager 1, which is an indication of the systematic uncertainty of the observations. **b**, Counting rate of particles triggering the electronic threshold of the first detector (L1) of some of the LETs and representing mainly ACR protons with  $\sim 0.5$ – $35$  MeV plus backgrounds of  $\sim 2$  s<sup>-1</sup> due to GCRs. **c**, Sum of three rates of GCR electrons with  $\sim 5$ – $45$  MeV observed by TET. The three rates in the sum are the ones labelled D13, D14 and D15 in Table 10 of Cummings et al.<sup>11</sup>, except that here the background has not been subtracted.

to a background of GCRs, as the heliosheath particles have escaped into interstellar space. In all the Voyager 2 rates shown, there are sudden increases of GCRs and decreases of ACRs during day 309 of 2018, indicating the crossing of the heliopause at 119.0 au, similar to the changes that occurred at Voyager 1 when it crossed the heliopause 6.2 yr earlier at 121.6 au.

Before the Voyager 1 crossing, the Voyager 1 rates showed evidence of interstellar flux tubes invading the heliosheath and providing a conduit for heliosheath particles to escape and an access point for GCRs to be observed in the heliosheath<sup>4</sup>. These intensity dropouts for ACRs and coincident increases for GCRs began  $\sim 14$  d and  $\sim 27$  d before the crossing and lasted a few days in each case. No such flux tubes were observed by Voyager 2 before its crossing of the heliopause. However, after Voyager 2 crossed the heliopause there are indications in Fig. 2 of layered step-like increases and decreases in the  $\sim 2$ – $100$  MeV GCR electron intensity that are anticorrelated with step-like changes in the  $0.5$ – $35$  MeV ACR proton rate. This anticorrelation somewhat resembles the anticorrelation in the changes of GCRs and ACRs in the Voyager 1 flux tubes observed during a 30 d period before crossing the heliopause, as seen in Fig. 1, where the GCRs increase when the ACRs decrease. We note that the pitch angles of particles entering LET A along its boresight, shown

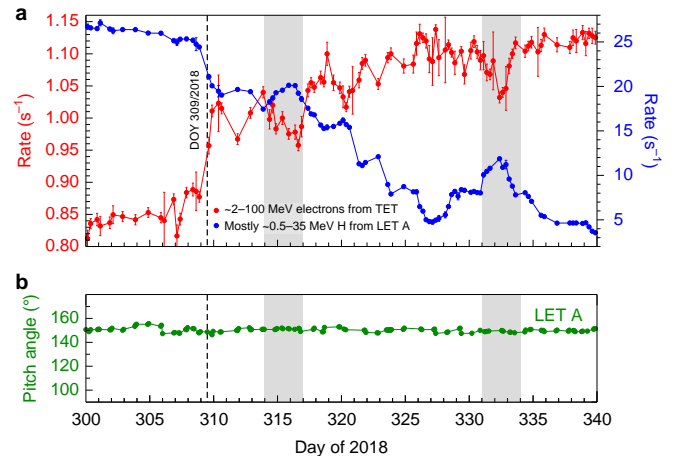


**Fig. 2 | Counting rates and particle pitch angles around the time of the Voyager 2 heliopause crossing.**

**a**, Counting rate of  $\sim 2$ – $100$  MeV GCR electrons from TET and  $\sim 0.5$ – $35$  MeV ACR protons from LET A (LA1 rate) for times just before and just after the Voyager 2 heliopause crossing on day 309 of 2018. The two shaded areas highlight two strong anticorrelations present in these two rates in the VLISM. Other significant anticorrelations are present, particularly evident in the period from day 310 to day 335. Both rates are 6 h averages. Error bars represent  $\pm 1$  s.d. **b**, Pitch angle of particles entering LET A along its boresight. The boresights of the two telescopes responsible for the rates, LET A and TET, are pointed in the same direction.

in Fig. 2b, are not significantly changing, compared with the  $120^\circ$  opening angle of the telescope, during the period after the heliopause crossing, so the variations seen in the electron and proton rates are not due to local changes in the magnetic field direction.

The transitions to the plateau level after the heliopause crossing took longer in the case of Voyager 2 versus Voyager 1 for the rates shown in Fig. 1, and they are similar in time for particles with very small gyroradii and much larger gyroradii. For example, a 5 MeV electron has a gyroradius of  $1.8 \times 10^{-4}$  au in a 0.7 nT magnetic field versus 0.030–0.036 au for a 380–540 MeV proton, which is approximately the range of median energies ascribed to the  $>70$  MeV H rate in Fig. 1 (ref. <sup>11</sup>). Thus, the longer transition time for Voyager 2 is not a gyroradius effect. However, the intensity of GCR protons with  $>70$  MeV and GCR electrons with  $\sim 5$ – $45$  MeV was only  $\sim 90\%$  of that observed 30 d later and further into interstellar space. Therefore, there is modulation of GCRs in a layer immediately beyond the heliopause. This layer has a similar extent to the layer in which ACRs are streaming outward along the interstellar magnetic field lines, as discussed below, suggesting the possibility that the anticorrelation in the rates arises from the interaction of the solar and interstellar magnetic fields back along the flank of the heliopause.

Streaming of the  $\sim 0.5$ – $35$  MeV protons is evident in Fig. 3 during the transition period after the heliopause crossing. LET A and LET C are mounted back to back, so differences indicate a streaming of particles. From day 255 of 2018 to approximately day 305, the rates are very nearly equal, indicating isotropy, but afterwards there are varying degrees of anisotropy until day 10 of 2019, when the rates drop to background levels. All three available rates from the front detector of the Voyager 2 LETs are shown in Fig. 3, along with the streaming index formed from the ratio of the hourly-averaged, background-corrected LC1-to-LA1 rates. The inset shows the telescope boresight components and the magnetic field components for 2018 day 310 in the  $N$ - $T$  plane of the  $RTN$  coordinate system. The  $RTN$  coordinate system is spacecraft centred, with  $R$  radially away from the Sun;  $T$  is parallel to the Sun's equator and in the direction of the Sun's rotation, and  $N$  completes the right-handed system.

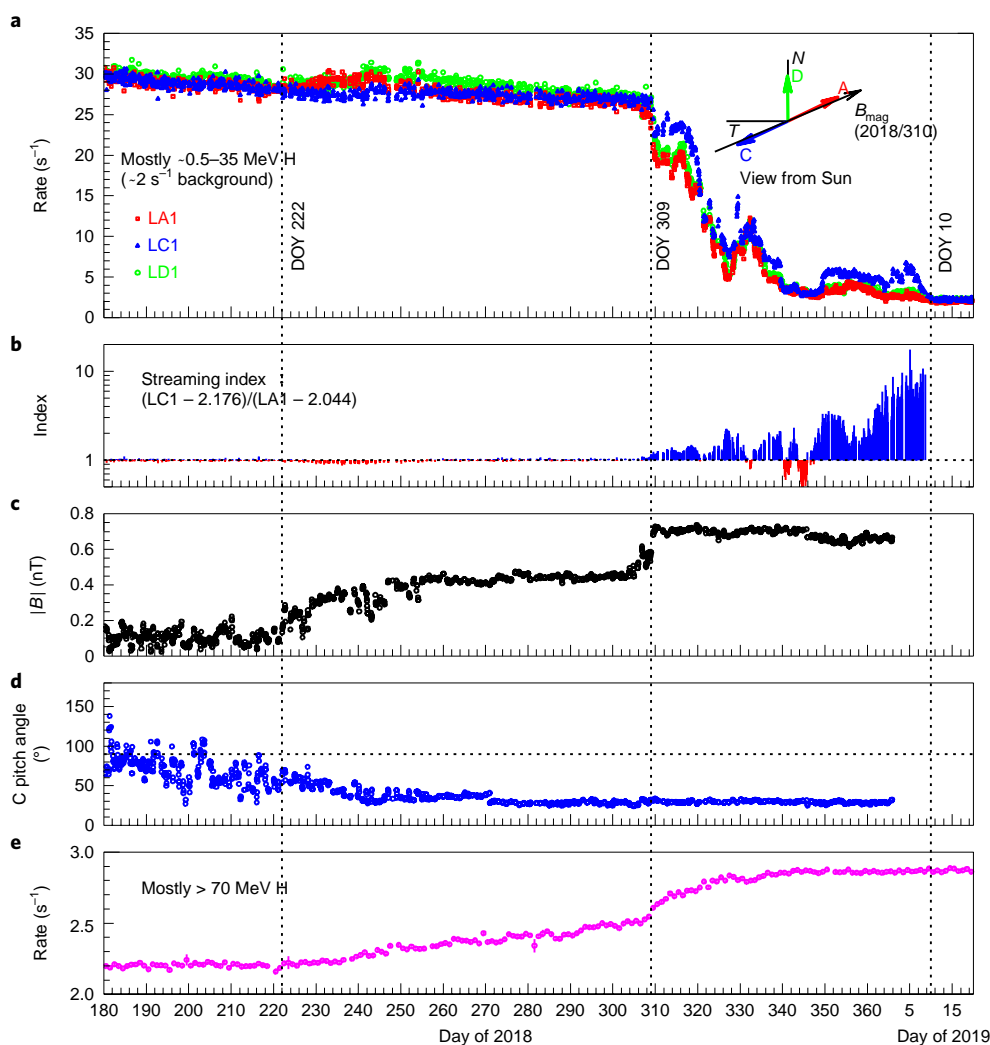


**Fig. 3 | Voyager 2 counting rates, streaming index, magnetic field strength and particle pitch angles for the period from day 180 of 2018 to day 20 of 2019.** **a**, Hourly-averaged counting rates from the first detector in each of three LETs, designated LA1, LC1 and LD1, which are dominated by  $\sim 0.5\text{--}35$  MeV protons plus backgrounds of  $\sim 2\text{ s}^{-1}$  due to GCRs. The inset shows the orientation of the telescopes' boresights in the  $N$ - $T$  plane along with the magnetic field direction in the same plane for day 310 of 2018. Error bars represent  $\pm 1$  s.d. **b**, Ratio of background-corrected rates of  $\sim 0.5\text{--}35$  MeV protons from LET C and LET A (uncorrected rates shown in **a**). The ratio is not plotted past 2019 day 10, the time at which the rates became background due to higher-energy GCRs. The background rates were calculated from days 16 to 22 of 2019. **c**, Hourly-averaged magnetic field strength. **d**, Pitch angle of particles entering LET C along its boresight plotted on an hourly basis. **e**, Daily-averaged rate of mostly  $>70$  MeV protons. It is the same as the V2 rate that is plotted in Fig. 1a except for a different time period. Error bars represent  $\pm 1$  s.d.

The direction of the magnetic field changes relatively little after the heliopause crossing<sup>13</sup>, so the inset is appropriate for the period beginning 2018/309 until the end of the magnetic field data. On the basis of the generally positive streaming during this period, it is likely that the particles are flowing along field lines that remain in contact with, or in close proximity to, the heliopause back along the flank of the heliosphere. This contact or proximity apparently abruptly ends on day 10 of 2019. Thus, the flow direction is consistent with Voyager 2 being on interstellar magnetic field lines in the VLISM that are connected to the heliopause further back along the flank of the heliosphere.

This cosmic ray boundary layer on the outside of the heliopause was not evident at the place and time where Voyager 1 crossed it, but this could be due to the different rates of separation of the heliopause from the spacecraft. Washimi et al.<sup>12</sup> used a three-dimensional model to calculate the positions of the heliopause versus time along the trajectories of both spacecraft and showed that Voyager 2 could

expect to remain closer to the heliopause after crossing than in the case of Voyager 1.

We note that the degree of streaming presented in Fig. 3 increases with time at the same time as the intensities are decreasing until day 10 of 2019, when the background level due to higher-energy GCRs is reached. This anticorrelation of the magnitude of the anisotropy with the intensity needs further study.

In both Figs. 1 and 3 there is evidence of another episode of anisotropy for the  $0.5\text{--}35$  MeV proton rates starting approximately on day 222 of 2018 (see also Fig. 4). This is approximately the same time that the  $>70$  MeV proton rate (Fig. 3e) begins to increase and also near the time at which Burlaga et al.<sup>13</sup> indicated that Voyager 2 had crossed into a magnetic barrier characterized by a region of increased magnetic field strength shown in Fig. 3c. As shown in Fig. 3e, the intensity of  $>70$  MeV protons began to increase at about this time and continued to rise steadily until the sudden jump at the heliopause crossing, indicating that a cosmic ray boundary

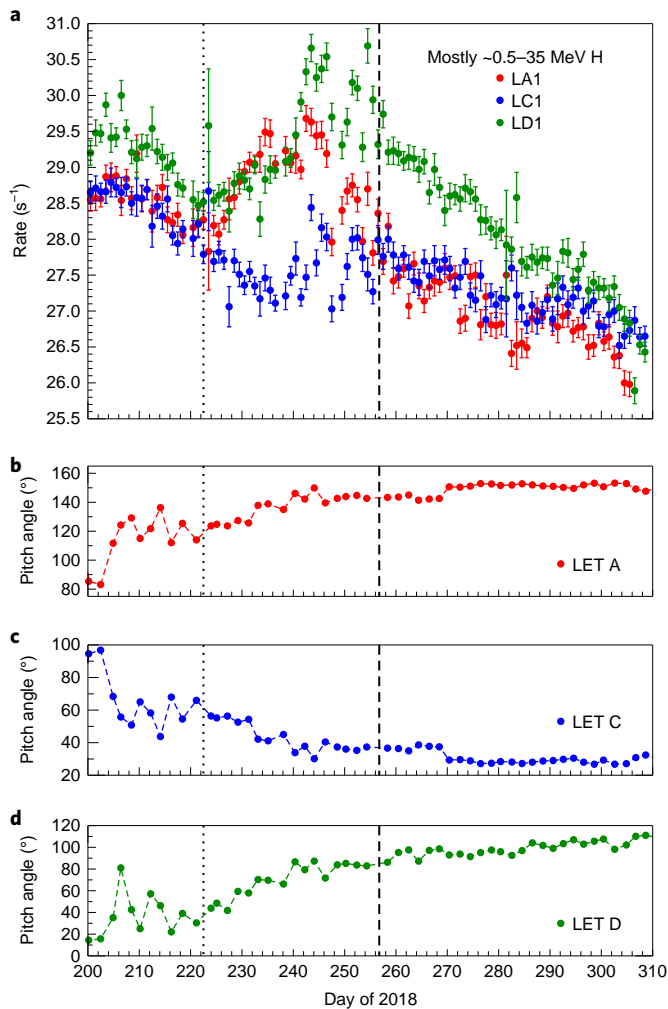


**Fig. 4 | Voyager 2 counting rates and particle pitch angles around the time of the particle anisotropy event.** **a**, The same as Fig. 3a except that the averaging is 1 d versus 1 h and the time period is day 200 to 310 of 2018, which provides a more detailed view of the anisotropy event that begins on day 222 at the beginning of the magnetic barrier. Error bars represent  $\pm 1$  s.d. **b–d**, Pitch angles of the particles entering the three telescopes along their boresights. The dashed vertical line denotes the time of a roll manoeuvre by the spacecraft to help calibrate the magnetometer. The dotted vertical line at day 222.5 indicates the beginning of the anisotropy event.

layer also exists on the inside of the heliopause. A similar gradient of GCRs before the heliopause crossing was present in the case of Voyager 1, as shown in Fig. 1.

In Fig. 4 we show the 0.5–35 MeV daily-averaged proton rates from day 200 to 310 of 2018, along with the pitch angles of particles entering the three telescopes along their boresights during this period, which includes the period of the magnetic barrier. The vertical line at day 222 marks the beginning of the anisotropy event, as evident by the change in trend of the LA1 rate, which we assume is the beginning of the magnetic barrier. The variation of the pitch angles is relatively smooth and small compared with the opening angle of  $120^\circ$  of the telescopes, and the anisotropy variation, though small, is significant and not smoothly varying, as evidenced by the behaviour of the rates before and after day 240. It appears that the local magnetic field is not governing the behaviour of the particles, suggesting that the anisotropies reflect conditions remote from the spacecraft.

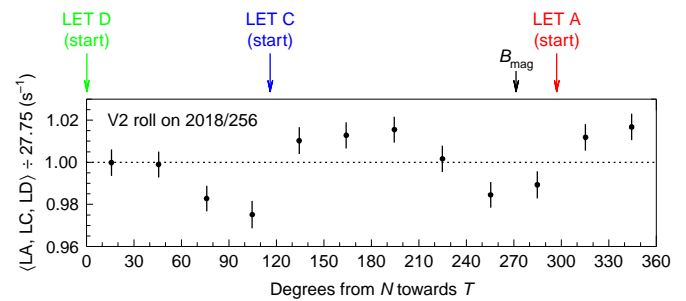


**Fig. 5 | Rate of ~0.5–35 MeV protons from Voyager 2 averaged over three telescopes (LETs A, C and D) during a spacecraft roll manoeuvre on day 256 of 2018.** The data are binned in  $30^\circ$   $N$ - $T$  angle bins and plotted at the average angle of the data within the bins. The angles in the  $N$ - $T$  plane of the boresights of the telescopes in the normal, fixed orientations are indicated, as is the direction of the magnetic field in the  $N$ - $T$  plane for the day of the roll. Error bars represent  $\pm 1$  s.d.

On day 256 of 2018, the Voyager 2 spacecraft executed a two-revolution roll about the  $R$  axis to help with the calibration of the magnetometer. This roll occurred in the middle of the anisotropy event; the time is shown as the vertical dashed line in Fig. 4. In Fig. 5 we show the average counting rate of  $\sim 0.5$ –35 MeV protons from the three telescopes in  $30^\circ$  bins from the  $N$  axis towards the  $T$  axis. There is a small but significant anisotropy, such that the intensity is largest in approximately the  $+N$  and  $-N$  directions ( $0$  and  $180$  on the horizontal axis), and thus represents a bidirectional pitch angle distribution, with the maximum intensity approximately perpendicular to the magnetic field direction. Note that this characterization of the anisotropy would be different for day 230, for example, since on that day the LA1 and LD1 rates are nearly the same, as shown in Fig. 4, whereas on day 256 LA1 and LC1 have nearly the same rate. Thus, the anisotropy is variable in the magnetic barrier.

When Voyager 1 crossed the heliopause, it was found that the transition to interstellar intensities had different timescales, depending on the pitch angle of the particles being observed and on the mass of the particles<sup>5</sup>. This is shown in Fig. 6a. ACR O nuclei with pitch angles near  $90^\circ$  persisted longer in the VLISM than did those with more field-aligned pitch angles<sup>5</sup>. Not shown in Fig. 6 but shown in Fig. 2 of Stone et al.<sup>5</sup> is that ACR O persisted longer than ACR He, which persisted longer than ACR H. This phenomenon was explained as being due either to a gradient drift in a non-uniform magnetic field<sup>6</sup> or to a particular pitch angle dependence of the perpendicular diffusion coefficient<sup>20</sup>. Fig. 6b shows that this phenomenon did not occur at Voyager 2. LET D in both the Voyager 1 and Voyager 2 cases had a telescope viewing angle to the magnetic field that encompassed  $90^\circ$ , and yet the behaviour is quite different. At Voyager 2, ACR O in LET D is similar to the average of LET A and LET C and the timescale for the transition is similar to that of 0.5–35 MeV protons as seen in Fig. 1. Thus, the conditions of a particular latitude gradient of the magnetic field strength or a particular form of the diffusion coefficient that led to the effects at Voyager 1 were not present at Voyager 2.

When Voyager 1 entered interstellar space there was no evidence of a significant gradient in the intensities of H in the VLISM along the trajectory of Voyager 1<sup>11</sup>. Voyager 2 is sampling a different region of the VLISM, being below the heliographic equator, whereas Voyager 1 is above it. At the time when Voyager 2 crossed the heliopause, the two spacecraft were 167 au apart. In Fig. 7 we show the energy spectra of H, He and electrons ( $e^+ + e^-$ ) from Voyager 2 for the period 2019/70–158 in the VLISM and compare them with the energy spectra of the same species from Voyager 1 in the VLISM<sup>11</sup>. The energy spectra in all cases are nearly identical. Thus,

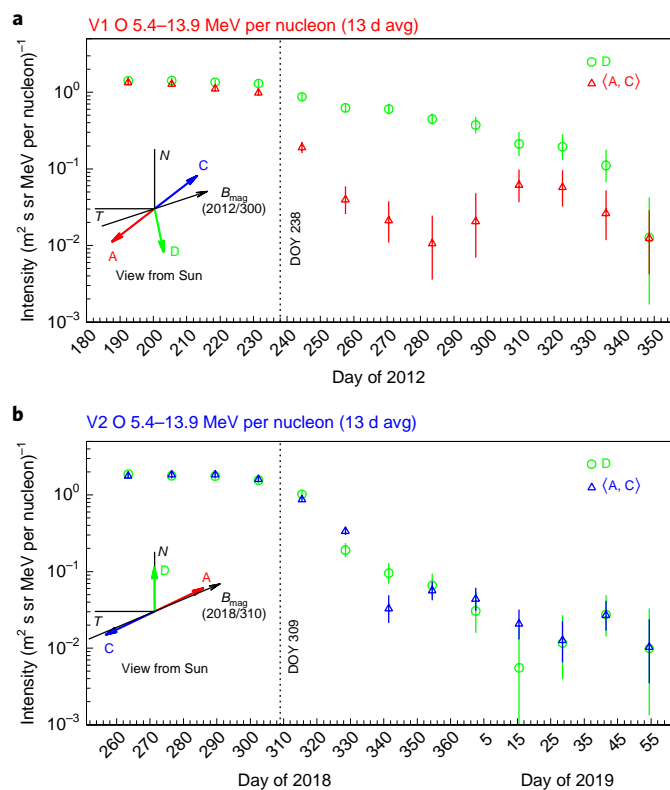


**Fig. 6** | Intensities of O nuclei with 5.4–13.9 MeV per nucleon in the vicinity of the Voyager 1 and Voyager 2 heliopause crossings. The symbol  $\langle A, C \rangle$  indicates an average of LET A and LET C intensities. The insets show the directions of the telescope boresights in the  $N$ - $T$  plane and the magnetic field direction in the same plane for specific days<sup>21,3</sup>. The dotted vertical lines show times of heliopause crossings. Error bars represent  $\pm 1$  s.d. **a**, Voyager 1. **b**, Voyager 2.

there is no significant gradient of the intensities across a wide region of the VLISM.

## Discussion

The crossings of the heliopause by the Voyager 1 and Voyager 2 spacecraft showed significant differences in the behaviour of the energetic particle populations. At Voyager 1, it appears that interstellar flux tubes had invaded the heliosphere and provided exit paths to the VLISM for ACRs and entrance paths from the VLISM for GCRs before the heliopause crossing. When Voyager 1 entered these flux tubes in the heliosheath, the result was occasional, strong anticorrelations in GCR and ACR particle intensities. Similar anticorrelations of ACRs and GCRs were seen at Voyager 2 but in the VLISM just past the heliopause rather than inside the inner heliosheath. This suggests that Voyager 2 may have been on magnetic field lines in the VLISM that were connected back to the flank of the heliopause. Supporting this concept was the observation of strong streaming of  $\sim 0.5$ – $35$  MeV protons along the magnetic field line for  $\sim 66$  d after the Voyager 2 heliopause crossing in the direction from the flank towards the nose of the heliosphere. The magnitude of the streaming is somewhat variable but generally increases with distance travelled by Voyager 2, although the intensity of the particles is decreasing. At the same time the magnetic field direction is not changing<sup>13</sup>, suggesting that the streaming is controlled by conditions at a remote source, presumably at the connection point to the heliopause.

There appear to be cosmic ray boundary layers on both sides of the heliopause, with the outer one only being evident at the position

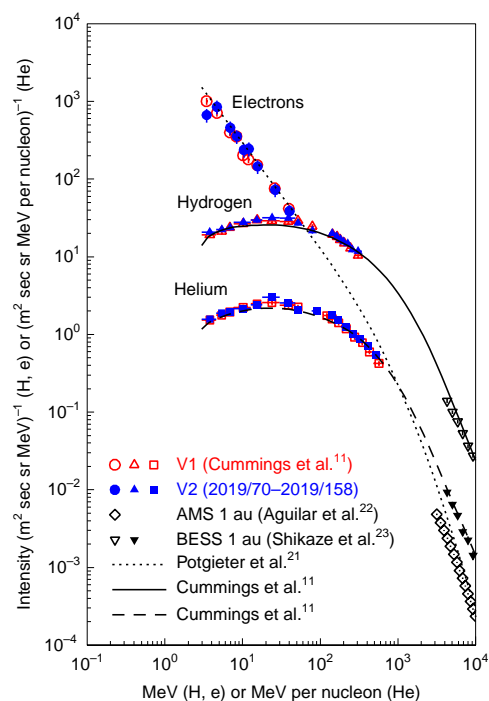


**Fig. 7** | Energy spectra of electrons ( $e^+ + e^-$ ), H nuclei and He nuclei observed by the CRS telescopes on Voyager 1 and Voyager 2. The Voyager 1 data are from Cummings et al.<sup>11</sup> and the descriptions and data sets used are described there. For Voyager 2, the same techniques were employed with slight differences described in Methods. The two lines labelled ‘Cummings et al.’ are from the GALPROP DR model and represent estimates of the interstellar spectra of H and He (ref.<sup>11</sup>). The dotted line is an estimate of the interstellar  $e^+ + e^-$  energy spectrum, which is identical to the estimate of the interstellar  $e^-$  energy spectrum of Potgieter et al.<sup>21</sup>. The higher-energy data are from ground-based observations<sup>22,23</sup>. Error bars represent  $\pm 1$  s.d.

of Voyager 2. In these layers the GCRs are modulated. In the case of Voyager 2, the layer on the inside of the heliopause coincides with the newly discovered magnetic barrier<sup>13</sup>, which is marked by a region of small but significant anisotropies of  $\sim 0.5$ – $35$  MeV protons.

In the case of the Voyager 1 crossing of the heliopause, there was a persistence of ACRs in the VLISM that depended on mass (heavier particles persisted longer) and on pitch angle (ones with pitch angles near  $90^\circ$  persisted longer). This effect was not seen at Voyager 2 and implies that the gradients of the magnetic field strength and/or the pitch angle dependences of the diffusion coefficient were different in the two cases<sup>6,20</sup>.

Comparison of the Voyager 1 and Voyager 2 energy spectra of H, He and electrons at two positions in the VLISM separated by  $\sim 167$  au shows that there is no significant intensity gradient of these particles over that region.

## Summary

The heliopause is the contact surface where the interstellar and solar plasmas meet at the outer boundary of the heliosphere. As Voyager 1 approached the heliopause in 2012, it found two regions where the interstellar magnetic field and GCRs had invaded the outer edge of the heliosphere, indicating a boundary that was more complex than a single, uniform contact surface. Voyager 2 did not find the same invasion six years later. Instead, it found a layered region in the local interstellar medium just outside the heliopause where the GCRs are modulated and the ACRs from inside are streaming outward along the interstellar magnetic field, which is

wrapped around the heliopause. There is more to be learned by continued observations of the VLISM and by further development of simulations and astrophysical applications.

## Methods

There are two types of CRS datum presented in this paper. The simplest type is the hardware rates, which consist of the counting rates of particles penetrating a single detector or multiple detectors in coincidence and leaving an ionization energy loss that exceeds hardware thresholds for each detector. These rates are shown in Figs. 1, 2a, 3a,e and 4a. In Fig. 5, hardware rates are also used but in this case the spacecraft is rotating and the data are collected into angle bins measured from the  $N$  axis towards the  $T$  axis in the  $RTN$  coordinate system before plotting.

The other type of datum consists of ‘pulse-height’ data. In addition to obtaining a count added to a rate counter when a particle deposits energy in a detector that exceeds a threshold value, in many cases a number from a pulse-height analyser is recorded that is related to the amount of energy deposited in a detector or combination of detectors. Using prelaunch calibrations, the pulse-height analyser numbers are converted to energy deposited in megaelectronvolts. Using techniques described in detail in Appendix A of Cummings et al.<sup>11</sup>, the energy spectra of different ions and of electrons shown in Fig. 7 were constructed, and the rates in various energy bins, as shown for example in Fig. 6, were produced.

There were some differences between the Voyager 1 and Voyager 2 analysis procedures. For example, for Voyager 2 all three LETs available were used for the ion spectra (LET A, LET C and LET D; LET B was damaged at the time of the Jupiter encounter in 1979) versus only LET C and LET D on Voyager 1. For the HET data, HET 1 was used on Voyager 2 versus HET 2 on Voyager 1. The electron spectra for Voyager 2 were constructed in the same way as described by Cummings et al.<sup>11</sup>, except that a 20% systematic uncertainty was added in quadrature to the statistical uncertainty of each rate instead of 10% in the case of Voyager 1. This resulted in the reduced chi squared of the fits being close to 1 in both cases.

## Data availability

Most of the CRS data can be obtained by clicking on the DATA link at <https://voyager.gsfc.nasa.gov/> and following other links to obtain rate and flux data. All data that were used in the figures can be provided by the corresponding author on request.

Received: 21 July 2019; Accepted: 27 September 2019;

Published online: 04 November 2019

## References

- Burlaga, L. F. & Ness, N. F. Voyager 1 observations of the interstellar magnetic field and the transition from the heliosheath. *Astrophys. J.* **784**, 146–159 (2014).
- Burlaga, L. F., Ness, N. F. & Stone, E. C. Magnetic field observations as Voyager 1 entered the heliosheath depletion region. *Science* **341**, 147–150 (2013).
- Gurnett, D. A., Kurth, W. S., Burlaga, L. F. & Ness, N. F. In situ observations of interstellar plasma with Voyager 1. *Science* **341**, 1489–1492 (2013).
- Krimigis, S. M. et al. Search for the exit: Voyager 1 at heliosphere's border with the galaxy. *Science* **341**, 144–147 (2013).
- Stone, E. C. et al. Voyager 1 observes low-energy galactic cosmic rays in a region depleted of heliospheric ions. *Science* **341**, 150–153 (2013).
- Florinski, V., Stone, E. C., Cummings, A. C. & le Roux, J. A. Energetic particle anisotropies at the heliospheric boundary. II. Transient features and rigidity dependence. *Astrophys. J.* **803**, 47–54 (2015).
- Strumik, M., Czechowski, A., Grzedzielski, S., Macek, W. M. & Ratkiewicz, R. Small-scale local phenomena related to the magnetic reconnection and turbulence in the proximity of the heliopause. *Astrophys. J. Lett.* **773**, L23–L27 (2013).
- Strumik, M., Grzedzielski, S., Czechowski, A., Macek, W. M. & Ratkiewicz, R. Advective transport of interstellar plasma into the heliosphere across the reconnecting heliopause. *Astrophys. J. Lett.* **782**, L7–L11 (2014).
- Strauss, R. D., Potgieter, M. S., Ferreira, S. E. S., Fichtner, H. & Scherer, K. Cosmic ray modulation beyond the heliopause: a hybrid modeling approach. *Astrophys. J. Lett.* **765**, L18–L23 (2013).
- Luo, X. et al. A numerical simulation of cosmic ray modulation near the heliopause. II. Some physical insights. *Astrophys. J.* **826**, 182–191 (2016).
- Cummings, A. C. et al. Galactic cosmic rays in the local interstellar medium: Voyager 1 observations and model results. *Astrophys. J.* **831**, 18–38 (2016).
- Washimi, H., Tanaka, T. & Zank, G. P. Time-varying heliospheric distance to the heliopause. *Astrophys. J.* **846**, L9–L14 (2017).
- Burlaga, L. F. et al. Magnetic field and particle measurements made by Voyager 2 at and near the heliopause. *Nat. Astron.* <https://doi.org/10.1038/s41550-019-0920-y> (2019).
- Gurnett, D. A. & Kurth, W. S. Plasma densities near and beyond the heliopause from the Voyager 1 and 2 plasma wave instruments. *Nat. Astron.* <https://doi.org/10.1038/s41550-019-0918-5> (2019).
- Krimigis, S. M. et al. Energetic charged particle measurements from Voyager 2 at the heliopause and beyond. *Nat. Astron.* <https://doi.org/10.1038/s41550-019-0927-4> (2019).
- Richardson, J. D., Belcher, J. W., Garcia-Galindo, P. & Burlaga, L. F. Voyager 2 plasma observations of the heliopause and interstellar medium. *Nat. Astron.* <https://doi.org/10.1038/s41550-019-0929-2> (2019).
- Stone, E. C. et al. Cosmic ray investigation for the Voyager missions: energetic particle studies in the outer heliosphere—and beyond. *Space Sci. Rev.* **21**, 355–376 (1977).
- Fisk, L. A., Kozlovsky, B. & Ramaty, R. An interpretation of the observed oxygen and nitrogen enhancements in low-energy cosmic rays. *Astrophys. J. Lett.* **190**, L35–L38 (1974).
- Pesses, M. E., Jokipii, J. R. & Eichler, D. Cosmic ray drift, shock wave acceleration, and the anomalous component of cosmic rays. *Astrophys. J. Lett.* **246**, L85–L89 (1981).
- Strauss, R. D. & Fichtner, H. Cosmic ray anisotropies near the heliopause. *Astron. Astrophys.* **572**, L3–L6 (2014).
- Potgieter, M. S., Vos, E. E., Munini, R., Boezio, M. & Di Felice, V. Modulation of galactic electrons in the heliosphere during the unusual solar minimum of 2006–2009: a modeling approach. *Astrophys. J.* **810**, 141–150 (2015).
- Aguilar, M. et al. Precision measurement of the ( $e^+ + e^-$ ) flux in primary cosmic rays from 0.5 GeV to 1 TeV with the Alpha Magnetic Spectrometer on the International Space Station. *Phys. Rev. Lett.* **113**, 221102 (2014).
- Shikaze, Y. et al. Measurements of 0.2–20 GeV/n cosmic-ray proton and helium spectra from 1997 through 2002 with the BESS spectrometer. *Astropart. Phys.* **28**, 154–167 (2007).

## Acknowledgements

We thank L. Burlaga for providing magnetic field data before publication. A.C.C. acknowledges support from the International Space Sciences Institute in Bern, Switzerland, to participate in the international team The Physics of the Very Local Interstellar Medium in the autumn of 2018. This work was supported by NASA under grant NNN12AA01C.

## Author contributions

All authors contributed to the production of this manuscript. A.C.C. and E.C.S. wrote the text. A.C.C., B.C.H. and N.L. performed the data analysis and A.C.C. and B.C.H. prepared the figures. All authors participated in reviewing and commenting on the paper and on the editor's and referees' comments.

## Competing interests

The authors declare no competing interests.

## Additional information

Correspondence and requests for materials should be addressed to E.C.S.

Peer review information *Nature Astronomy* thanks Horst Fichtner and the other, anonymous, reviewer(s) for their contribution to the peer review of this work.

Reprints and permissions information is available at [www.nature.com/reprints](http://www.nature.com/reprints).

Publisher's note Springer Nature remains neutral with regard to jurisdictional claims in published maps and institutional affiliations.

© The Author(s), under exclusive licence to Springer Nature Limited 2019